U. of Iowa 67-36

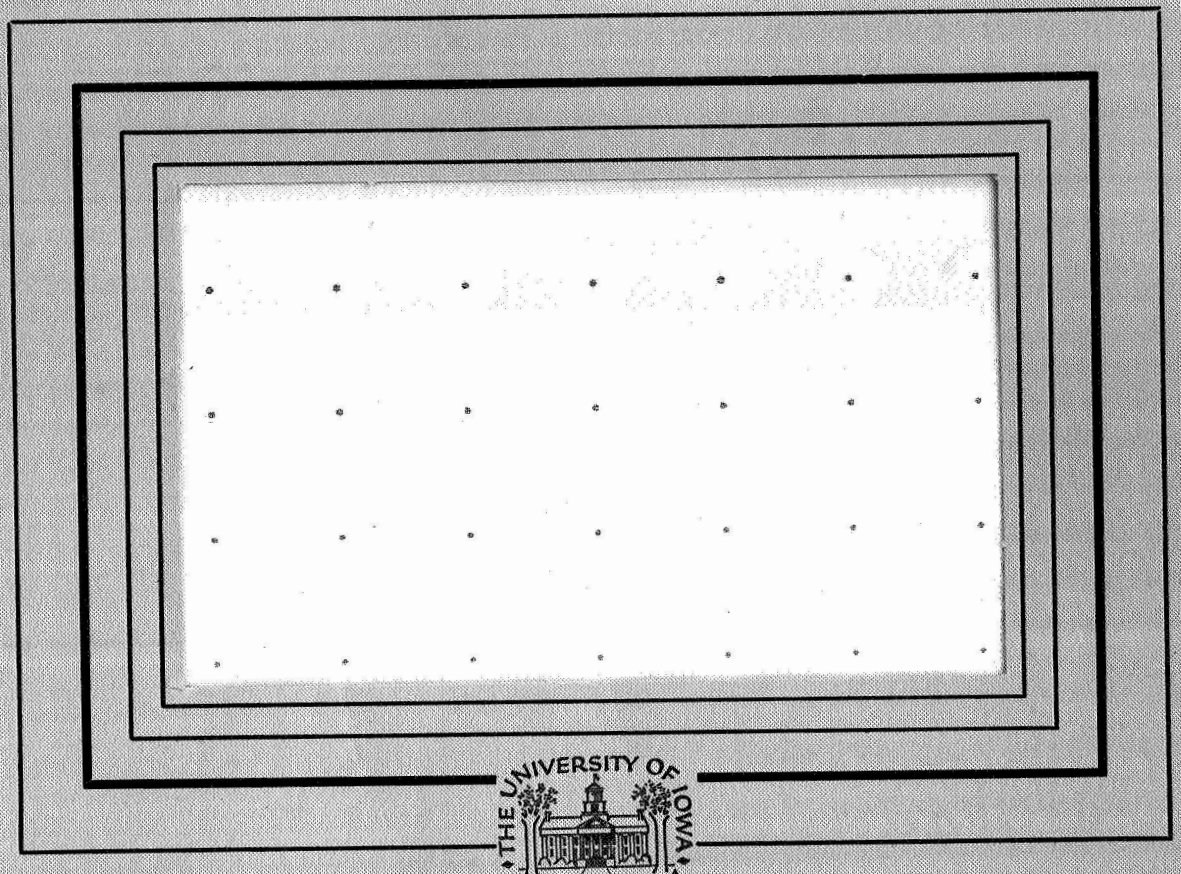

Department of Physics and Astronomy

THE UNIVERSITY OF IOWA

Iowa City, Iowa

RECENT OBSERVATIONS OF LOW-ENERGY CHARGED PARTICLES IN THE EARTH'S MAGNETOSPHERE*

by

L. A. Frank

July, 1967

Department of Physics and Astronomy
University of Iowa
Iowa City, Iowa

*This research was supported in part by the National Aeronautics and Space Administration under Grant NsG-233-62 and Contract NAS5-2054 and by the Office of Naval Research under Contract Nonr-1509(06). Paper presented at the Summer Institute on Physics of the Magnetosphere, Boston College, June, 1967.

ABSTRACT

Several recent observations of low-energy proton and electron intensities within the energy range ~ 100 eV to 50 keV in the earth's radiation zones with a sensitive array of electrostatic analyzers borne on the earth-satellite OGO 3 during mid-1966 are summarized. Measurements of charged particles of the extraterrestrial ring current during a moderate geomagnetic storm, of the low-energy proton and electron distributions in the vicinity of the midnight 'trapping boundary' near the magnetic equatorial plane, and of upper limits for proton and ion (100 eV $\leq \frac{E}{Q} \leq$ 50 keV) energy fluxes deep within the inner radiation zone are presented together with several introductory comments concerning the morphology of the omnidirectional intensities of energetic electrons ($E \geq 40$ keV, ≥ 230 keV and ≥ 1.6 MeV) at the magnetic equator in the outer radiation zone.

INTRODUCTION

A large collection of detailed observations of energetic charged particles within the vast region encircling the earth which is dominated by the geomagnetic field has been acquired since the initial discovery of intense fluxes of energetic protons and electrons in these regions, the inner and outer radiation zones, with earth-satellite measurements in 1958. Current reviews concerning the observations of electrons $E \gtrsim 10$ keV and of protons $E \gtrsim 100$ keV with instrumentation borne on earth-orbiting satellites at low and high altitudes, ~ several hundred kilometers to 30 R_E (R_E, earth radius), have been published over the past several years [Van Allen, 1963; O'Brien, 1964a; Frank and Van Allen, 1964; Shabansky, 1965; Hess, 1965; Frank, 1965a]. Although the major fraction of the literature has been directed toward detailed studies of electron and proton intensities in the above energy ranges within the earth's radiation zones, lower energy charged particles with energies $E \lesssim 10$ keV dominate these regions in terms of energy densities and number densities. For example, the ratios of the number densities and energy densities of the often-observed electron ($E \gtrsim 1$ MeV) intensities in the heart of the outer radiation zone near the magnetic equatorial plane at 4.5 R_E to the corresponding number and energy densities of electrons ($E \lesssim 10$ keV) are frequently $\sim 3 \times 10^{-6}$ and 2×10^{-3}, respectively. Although these energetic

charged particle distributions have been and are presently being thoroughly surveyed via in situ measurements, the observations of lower energy charged particles are limited not through oversight of the importance of their distributions throughout the magnetosphere but due to the difficulties of designing instruments with sufficient sensitivity, energy thresholds and immunity from background responses attributable to penetrating, energetic charged particles and to ultraviolet radiations. Recently observations of low-energy proton and electron intensities over the energy range extending from ~ 100 eV to 50 keV have been obtained in the earth's radiation zones near the magnetic equatorial plane with a sensitive array of electrostatic analyzers borne on the satellite OGO 3 [Frank 1967a, b, c; Frank and Swisher, 1967]. These measurements and several unpublished, preliminary results concerning the extraterrestrial ring current, the possible existence of large energy fluxes of low-energy positive ions deep within the earth's inner radiation zone, and the structure of the "trapping" boundary at ~ 8 R_E geocentric radial distance in the midnight meridional plane together with several introductory comments concerning the distributions of energetic electrons ($E \gtrsim 40$ keV) in the outer radiation zone are presented herein as a summary of initial, unique observations of the low-energy charged particle distributions within the earth's radiation zones.

SEVERAL COMMENTS ON THE DISTRIBUTIONS OF ENERGETIC ELECTRON INTENSITIES IN THE OUTER RADIATION ZONE

As was mentioned earlier the energetic charged particle populations of the inner and outer radiation zones have been under intensive examination during the past several years. Comprehensive surveys with Geiger-Mueller tubes, scintillators, and solid-state devices are available for regions near the magnetic equatorial plane throughout the radiation zones, at low altitudes ($\sim$ 1000 km) from equator to poles, and for the entire inner radiation zone within the energy ranges $E \gtrsim 100$ keV for protons and $E \gtrsim 50$ keV for electrons [cf McIlwain, 1963; Frank, 1965a, Frank, Van Allen and Hills, 1964; Davis, 1965; Freden, Blake and Paulikas, 1965; Gabbe and Brown, 1966; Vette, 1966]. One of the principal observational tasks is the organization of a massive abundance of measurements into a coherent, concise description of the complex species - and energy-dependent morphology of the earth's radiation zones. An example of the morphology of energetic electron intensities in the outer radiation zone at the magnetic equator is shown in Figures 1 and 2 [Owens and Frank, 1967] which summarize four months of observations of electron ($E \geq 40$ keV, ≥ 230 keV and ≥ 1.6 MeV) intensities with an array of Geiger-Mueller tubes borne on Explorer 14 during the period beginning at launch on 2 October 1962 through January 1963 (refer to Frank,

Van Allen and Hills [1964] for details concerning instrumentation and orbital parameters). Of immediate interest are the orbital inclination 33°, initial apogee geocentric radial distance 16.4 R_E, initial perigee altitude 281 kilometers and period 36.4 hours. Figures 1 and 2 summarize contours of constant omnidirectional intensities of electrons with energies exceeding the above detector thresholds as functions of L and time at the magnetic equator. The daily sum K_p, ΣK_p, has been included at the bottom of each of these graphs in order to indicate periods of relative magnetic activity. Several features of the morphology of these energetic electron intensities are immediately evident upon perusal of these graphic summaries: (1) the apparent complexity of the temporal variations and the dependence of the gross temporal behavior upon electron energy, (2) the increases of electron intensities following the onset of a period of relative magnetic disturbance (high ΣK_p) with peak values of omnidirectional intensities occurring with increasing time delay after onset of the disturbance with increasing electron energy (refer to the late December 1962 enhancements for a clear example), (3) the ebbing of the intensities of electrons ($E \geq 230$ keV and ≥ 1.6 MeV) during a sustained period of relative magnetic quiescence beginning 23 December through 9 January, (4) the sudden decreases of electron (in particular $E \geq 1.6$ MeV) intensities concurrent with the onset of magnetic disturbance and (5) the persistent occurrence of <u>peak</u> electron ($E \geq 230$ keV and ≥ 1.6 MeV)

omnidirectional intensities at $L \simeq 4.5$ to 5.5 and of peak electron ($E \geq 40$ keV) intensities over a relatively broad L-value range $L \simeq 4$ to 7. Many of these observations have been reported previously [cf Frank, Van Allen and Hills, 1964; Frank, 1965a, b, c] but this presentation provides the most comprehensive panorama of the Explorer 14 measurements presently available and offers rapid insight into the complex temporal behavior of outer zone electron intensities. Although several of the temporal variations in intensities evident in Figures 1 and 2 may be at least in part understood without knowledge of the dominant lower energy particles (for example, inward radial diffusion [Frank, 1965b] and adiabatic relocation and acceleration due to an enhanced extraterrestrial ring current during magnetic storms [McIlwain, 1966]), a complete theoretical investigation depends heavily upon a thorough analysis of the low-energy particle populations throughout these regions. Several initial observations of these low-energy charged particle intensities are discussed in the following summaries.

UPPER LIMITS FOR THE ENERGY FLUXES OF LOW-ENERGY PROTONS AND IONS IN THE INNER RADIATION ZONE

Early low-altitude surveys of the energy fluxes of low-energy protons or ions within the energy range extending from ~ 500 eV to 1 MeV with an array of CdS crystals borne on the low-altitude satellite Injun 1 provided the remarkable result that large energy fluxes, ~ 50 ergs $(cm^2\text{-sec-sr})^{-1}$, were present deep within the inner radiation zone at $1.25 \lesssim L \lesssim 1.70$ [Freeman, 1962]. A summary of these observations in a B-L coordinate system is included in Figure 3. These measurements implied a strong acceleration mechanism for protons or positive ions within a region which is deeply imbedded within the earth's magnetosphere, and hence presumably relatively remote from the outer magnetosphere where the solar wind is an able energy source for charged particle acceleration. An order-of-magnitude estimate of the source strength necessary to maintain these energy fluxes may be easily obtained by assuming that (1) the charged particles are ~ 1 keV protons, (2) the fluxes are confined to a volume bounded by the L-shells 1.25 and 1.70 and a spherical surface at ~ 1000 km altitude above the earth's surface and (3) the principal loss mechanism is charge-exchange (although Coulomb scattering is a loss mechanism of similar magnitude for protons in this energy range) in the ambient terrestrial exosphere [Liemohn, 1961]. This estimate of the power required to maintain these energy

fluxes is 10^{18} ergs(sec)$^{-1}$ which is comparable to the average source strength necessary for electron precipitation into the auroral regions [cf Frank and Van Allen, 1964; O'Brien, 1964b].

Recently we have searched for these energy fluxes of low-energy protons or ions with the array of sensitive electrostatic analyzers which was included on the OGO 3 spacecraft (launch date, 7 June 1966; initial apogee and perigee 128,500 km and 6,700 km geocentric radial distances; inclination, 31°) and were unable to discern any signature of large positive or negative ion intensities within the energy range 100 eV $\leq \frac{E}{Q} \leq$ 50 keV in the region of the inner radiation zone surveyed with Injun 1 [Frank and Swisher, 1967]. In fact the responses of the electrostatic analyzers were unmodulated by the variations in curved-plate potential and are background counting rates attributable to penetrating, energetic protons and electrons. Hence only upper limits for the energy fluxes of protons or positive ions (100 eV $\leq \frac{E}{Q} \leq$ 50 keV) were generously determined by assuming that these background responses were wholly due to low-energy ion fluxes. The corresponding upper limits for these energy fluxes are summarized in Figure 3 in order to facilitate comparison of the two results. All measurements reported in the present discussion were obtained at local pitch angles $\alpha = 90°$. A cursory examination of Figure 3 shows that the OGO 3 upper limits for energy fluxes of protons or positive ions (100 eV $\leq \frac{E}{Q} \leq$ 50 keV) are less than the Injun 1 measurements by factors ~ 10 to 100. Upper limits for <u>negative-ion</u> (100 eV $\leq \frac{E}{Q} \leq$ 50 keV) energy fluxes as derived

from the responses of companion electron electrostatic analyzers are within a factor ~ 2 equal to the simultaneously measured upper limits for positive-ion energy fluxes reported here. It is possible that the energy fluxes observed with Injun 1 are predominantly shared by protons with energies exceeding the energy range of the OGO 3 electrostatic analyzers, the energy range 50 keV $\lesssim$ E $\lesssim$ 1 MeV. In order to investigate this possibility we have examined Injun 4 (launch, 21 November 1964; initial apogee and perigee altitudes, 2502 km and 527 km; inclination, 81°) observations of energy fluxes of protons within the energy range extending from ~ 30 keV to 4.2 MeV and have summarized the results in Table I. Again there is no evidence of a large energy flux, ~ 50 ergs $(cm^2\text{-sec-sr})^{-1}$, of protons in this energy range.

It is possible that (1) the large energy fluxes of positive ions are present only near local midnight where all Injun 1 measurements were obtained [Freeman, 1962] and hence that the OGO 3 observations during local day simply imply that these low-energy positive ions are confined to a restricted local-time range centered near local midnight (the Injun 4 measurements were also acquired near local midnight) or (2) these low-energy positive ions have disappeared via an occasional loss mechanism over the period extending from mid-1961 (Injun 1) to mid-1966 (OGO 3). However, on the basis of the above findings of firm upper limits for these energy fluxes which are less

TABLE I

SEVERAL UPPER LIMITS FOR ENERGY FLUXES
OF PROTONS IN THE EARTH'S INNER RADIATION ZONE*

INJUN 4

January 1965

L, earth radii	B, gauss	Energy Flux+ (upper limits), $erg(cm^2\text{-}sec\text{-}sr)^{-1}$	
		protons $E > 30$ KeV	protons $0.5 \leq E \leq 4.2$ MeV
1.35	0.151	2.5	5×10^{-4}
1.49	0.182	0.2	6×10^{-3}
1.50	0.167	1.5	- - -
1.51	0.170	1.0	2.6×10^{-4}
1.55	0.179	0.7	1.4×10^{-2}

*See also Frank and Swisher [1967].

+At local pitch angle $\alpha = 90°$.

by factors of 10 to 100 when compared with the energy fluxes reported by Freeman over a large region of the inner zone, we conclude that most probably energy fluxes of protons or ions (500 eV $\lesssim$ E $\lesssim$ 1 MeV), $\sim$ 50 ergs $(cm^2\text{-sec-sr})^{-1}$, are not a feature of the inner radiation zone.

FIRST OBSERVATIONS OF CHARGED PARTICLES OF THE EXTRATERRESTRIAL RING CURRENT DURING GEOMAGNETIC STORMS

The search for a large ring current of charged particles encircling the earth, which was early postulated as the phenomenon responsible for the sporadic occurrences of rapid world-wide decreases of the magnetic field intensity over low and middle latitudes at the earth's surface [Chapman and Ferraro, 1932], has continued since the discovery of the earth's radiation zones. Recently the magnetic 'signature' of this extraterrestrial ring current in the outer radiation zone has decisively been discerned with *in situ* measurements of the vector magnetic field via a satellite-borne magnetometer [Cahill 1966]; these measurements positioned the center of this ring current near 3.5 R_E in the magnetic equatorial plane during a great magnetic storm. The direct detection of the charged particles of the extraterrestrial ring current has been obstructed until recently due to rigorous requirements upon detector energy thresholds, sensitivities and immunity to a variety of background responses. Several principal results of the first observations of the charged particle distributions within the extraterrestrial ring current during a moderate geomagnetic storm [Frank, 1967c] are summarized in the following discussion.

The hourly $D_{ST}(H)$ values for a moderate ($\sim -50\gamma$) geomagnetic storm during early-July 1966 and corresponding perigee passages

designated as 'P', during which 'snapshots' of the radial profiles of charged particle intensities over similar low-latitude traverses of the radiation zones with OGO 3 are available, have been summarized in Figure 4. The corresponding four 'snapshots' of the proton ($31 \leq E \leq 49$ keV) directional intensities as functions of L during pre-storm (7 July), main phase (9 July), recovery (11 July) and post-storm (13 July) conditions are plotted in Figure 5 with equal ordinate scales in order to facilitate comparison of intensities; at a given L-value there is no significant difference in latitude of the spacecraft position or directions of the fields of view of the electrostatic analyzers for these four passes. Hence all variations in intensities at a given L-value as displayed in Figure 5 are temporal and directly correlated with the magnitude of $D_{ST}(H)$. It is of interest to note that the maximum proton ($31 \leq E \leq 49$ keV) intensity observed during the main phase of this moderate magnetic storm is 7.4×10^{7} $(cm^{2}\text{-sec-sr})^{-1}$ and is located at $L = 3.6$ in gross agreement with the position of the center of the ring current as inferred from in situ magnetic field measurements during another geomagnetic storm [Cahill, 1966].

In order to establish that the proton (200 eV $\lesssim E \lesssim 50$ keV) intensities are indeed the predominant contributors to the extraterrestrial ring current, it is not only necessary to demonstrate the above positive correlation of their intensities with the magnitude of the depression of the field intensity at the surface of the earth,

$D_{ST}(H)$, but also to show that the energy reservoir of this population of charged particles in the outer radiation zone is of sufficient magnitude to account for the observed $D_{ST}(H)$. Toward the goal of calculating the total energy of low-energy protons and electrons in the outer radiation zone we have computed the energy densities of protons and electrons (200 eV $\leq$ E $\leq$ 50 keV) as functions of shell-parameter L observed over the low-latitude ($|\lambda_m| < 20°$) traversal of OGO 3 through the radiation zones during the main phase of the geomagnetic storm on 9 July and have displayed these results in Figure 6 accompanied with the magnetic energy density, $B^2/8\pi$, as calculated by invoking a magnetic field model derived from surface measurements of the terrestrial magnetic field [Jensen and Cain, 1962]. Note that the peak proton (200 eV $\leq$ E $\leq$ 50 keV) energy density exceeds the peak electron (200 eV $\leq$ E $\leq$ 50 keV) energy density by a factor $\sim$ 7 and that the sharp onset of the near-earth decline of proton (200 eV $\leq$ E $\leq$ 50 keV) energy densities at L = 3.2 is deeper within the outer radiation zone than the corresponding decrease in electron (200 eV $\leq$ E $\leq$ 50 keV) energy densities at L = 4.0. Both of these observations should eventually be significant in delineating the principal acceleration mechanism for the large enhancements of these low-energy charged particles.

The decrease of the terrestrial magnetic field intensity on the geomagnetic equator at the earth's surface, $\Delta B(o)$, is proportional to the total energy of these low-energy charged particles [Dessler and

Parker, 1959] or, explicitly, in the linear theory

$$\Delta B(o) = - 2.6 \times 10^{-21} \mathcal{E} \text{ gammas}$$

where $\mathcal{E}$ is the total energy of the charged-particle population in units of ergs [Sckopke, 1966]. In order to evaluate the total energy of the low-energy proton and electron distributions it is necessary to expand the 'snapshots' of Figure 6 into meridional cross-sections of the energy density contours in a R-λ_m coordinate system by approximating the latitude dependence of the energy densities, W, via utilization of simultaneous observations of the directional intensities at two pitch angles at a given L-value with the power law

$$W(L, B) = K(L) \left(\frac{B}{B_o}\right)^{-n} \quad \text{erg(cm)}^{-3}$$

where n is n(L) and typically $1(\pm 0.5)$. The reader is referred to a detailed discussion given by Frank [1967c] for observational justification of this approximation. An example of the contours of constant energy densities of protons ($200 \text{ eV} \leq E \leq 50 \text{ keV}$) during the main phase of the moderate geomagnetic storm of early-July is presented in Figure 7. The total energy of low-energy protons, $\mathcal{E}_p$, within the earth's radiation zones over L = 1 to 8 and under the assumption that the ring current is <u>symmetric</u> [cf Akasofu and Chapman, 1964; Cahill, 1966] becomes

$$\mathcal{E}_p = 3.24 \times 10^{27} \int_1^8 \int_o^{\lambda_c} K(L)\, L^2 (\cos^{6n+7}\lambda)\, (4-3\cos^2\lambda)^{-n/2}\, dL d\lambda \text{ ergs}$$

where $K(L)$ is the equatorial energy density at L in $erg(cm)^{-3}$,

$n = n(L)$ is the exponent of the latitude dependence of W_p above,

λ denotes magnetic latitude,

$\lambda_c = \text{Arccos}\left(\frac{1}{L}\right)^{1/2}$ and

L is in units of earth radii.

Attention is drawn upon the fact that the B-L coordinate system derived from a magnetic field model based upon surface measurements of the terrestrial magnetic field is used as a reference coordinate system throughout the above presentations and calculations. Clearly the observed relatively high, energy densities of charged particles reported here will significantly distort the geomagnetic field especially at the position of the ring current. A tabular comparison of the calculated and the observed decreases, $\Delta B(o)$ and $D_{ST}(H)$, respectively, of the magnetic field intensity at the earth's surface near the equator, neglecting the diamagnetism of the earth, for the main phases of two moderate magnetic storms and a typical quiescent period is provided in Table II. The calculated charged-particle total energies, and hence the calculated $\Delta B(o)$, are judged to be accurate to within $\pm$ 50% (refer to Frank [1967c]). Inspection of the calculated and observed magnitudes of the decreases of field intensities at the earth's surface shown in Table II firmly establishes that (1) protons ($200\ eV \lesssim E \lesssim 50\ keV$) are the principal contributors to the storm-time extraterrestrial ring current and

TABLE II

REPRESENTATIVE TOTAL PROTON ($200\ eV \leq E \leq 50\ keV$) AND ELECTRON ($200\ eV \leq E \leq 50\ keV$) ENERGIES WITHIN THE EARTH'S RADIATION ZONES*

Date	Charged Particles	Charged Particle Total Energy $1 \leq L \leq 8$ (ergs)	$\Delta B(o)$ Calculated (gammas)	$D_{ST}(H)$ Observed (gammas)
23 June 1966	Protons ($200\ eV \leq E \leq 50\ keV$)	4.8×10^{21}	-12	Quiescent
25 June 1966	Protons ($200\ eV \leq E \leq 50\ keV$)	1.4×10^{22}	-36	-30($\pm$10)
9 July 1966	Protons ($200\ eV \leq E \leq 50\ keV$)	2.1×10^{22}	-55	-50($\pm$10)
	Electrons ($200\ eV \leq E \leq 50\ keV$)	5.3×10^{21}	-14	

*See also Frank [1967c].

(2) electrons (200 eV $\lesssim$ E $\lesssim$ 50 keV) are substantial, though lesser, contributors, ~ 20% of the total ring current, a result which is in qualitative agreement with earlier measurements with CdS crystals borne on Explorer 12 [Frank, 1966b].

ON THE DISTRIBUTIONS OF LOW-ENERGY PROTONS AND ELECTRONS IN THE VICINITY OF THE 'TRAPPING BOUNDARY' NEAR THE MAGNETIC EQUATOR

Detailed observations of the electric fields, magnetic fields and charged particle distributions within the earth's magnetosphere are necessary in order to delineate the predominant acceleration mechanism(s) providing the large intensities of low-energy protons and electrons which populate the radiation zones and their environs. A host of possible mechanisms and reasonable models have been proposed (cf Axford and Hines, 1961; Alfvén and Fälthammar, 1963; Dessler, Hanson and Parker, 1961; Block, 1966; Kennel and Petschek, 1966; Taylor and Hones, 1965]; several initial observations of low-energy protons and electrons which are pertinent to the phenomenon of local acceleration of charged particles within the outer magnetosphere are presented here.

Our first efforts toward developing a description of the morphology of the low-energy proton and electron (200 eV $\leq$ E $\leq$ 50 keV) distributions within the outer magnetosphere as measured with the OGO 3 electrostatic analyzer array have established several salient features of the intensity distributions at the 'trapping boundary' at local midnight near the magnetic equatorial plane. A typical set of profiles of low-energy electron intensities as functions of shell-

parameter L, again calculated with Jensen and Cain [1962] coefficients for the geomagnetic field, are displayed in Figure 8 during an inbound pass through the outer magnetosphere at low magnetic latitudes near the midnight meridional plane ($\varphi_{SM} = 180°$). These profiles of the directional intensities of electrons ($630 \leq E \leq 1100$ eV, $1.5 \leq E \leq 2.7$ keV, $6.8 \leq E \leq 12$ keV, $27 \leq E \leq 47$ keV and $E > 45$ keV) are remarkably dissimilar with the exception of the region below $L \simeq 5$ in the outer radiation zone and are typical of the observed distributions of intensities in this region. The position of the sharp decrease in electron ($E > 45$ keV) intensities with increasing L at $L \simeq 7.0$ has often been termed the 'trapping boundary' [cf Frank 1965a; Craven 1966] in the local-night hemisphere of the magnetosphere at high and low magnetic latitudes; whether or not it is in fact the outermost limit of durable trapping within the earth's magnetosphere as suggested by the above designation is a problem which remains unresolved. Inspection of Figure 8 reveals the distributions of lower energy electron intensities are positioned with respect to the 'trapping boundary' via a complex and energy-dependent relationship for $L \gtrsim 5$: (1) only a small variation of electron ($27 \leq E \leq 47$ keV) intensities occurs at the 'trapping boundary' coincident with the onset of a large decrease in electron ($6.8 \leq E \leq 12$ keV) intensities with decreasing L, (2) a rapid decrease of intensities of electrons ($1.5 \leq E \leq 2.7$ keV) with decreasing L-value at $L = 6.0$ <u>inside</u> the

'trapping boundary' and (3) a small maximum of electron ($630 \leq E \leq 1100$ eV) intensities inside the 'trapping boundary'. We shall direct our attention herein primarily to the positions of the onset of the near-earth decreases of electron intensities and designate these positions as $L_D(E)$. A series of observations over similar traversals of this region are displayed in Figures 9, 10 and 11. For a given L-value the coordinates α_o (equatorial pitch angle), φ_{SM} (solar magnetospheric longitude) and λ_m (geomagnetic latitude) during this period do not largely differ from those plotted in Figure 8 since the orbital period of the spacecraft is 48.6 hours (2.03 days). A striking feature of the observations during these four passes is the persistent deeper penetration of maximum electron ($1.5 \leq E \leq 2.7$ keV) intensities when compared to the corresponding near-earth onset of decreasing intensities of electrons ($3.8 \leq E \leq 6.8$ keV), or in our notation L_D ($1.5 \leq E \leq 2.7$ keV) $< L_D$ ($3.8 \leq E \leq 6.8$ keV). A definite position of the onset of a sharp decrease in electron ($14 \leq E \leq 24$ keV) intensities is not usually cognizable but is positioned at $L_D(14 \leq E \leq 24$ keV) $> L_D(3.8 \leq E \leq 6.8$ keV) when a decrease is apparent (cf Figure 10). The persistent occurrence of greater values of $L_D(E)$ with increasing electron energy within the energy range ~ 1 to 10 keV is demonstrated by the summary offered in Table III which includes K_p for the period of observation of L_D and the corresponding daily sum K_p, ΣK_p [Lincoln, 1966]. The values of L_D vary by several earth radii within the series

TABLE III

OBSERVED VALUES OF THE PARAMETER $L_D(E)$
NEAR THE MIDNIGHT MERIDIONAL PLANE

Date (inbound pass)	$L_D(1.5 \leq E \leq 2.7$ keV), earth radii	$L_D(3.8 \leq E \leq 6.8$ keV), earth radii	K_p during observation of L_D	Daily Sum K_p (ΣK_p)
27 June 1966	6.2	6.7	0^+	7^-
29 June 1966	7.2	7.5	1^-	11^+
1 July 1966	5.3	5.9	1^+	12^-
3 July 1966	8.4	8.7	1^-	9^+

of observations reported here and display no obvious correlation with K_p or ΣK_p, but the difference $L(3.8 \leq E \leq 6.8$ keV) - $L(1.5 \leq E \leq 2.7$ keV) is usually $\sim 0.5\ R_E$. During the main phase of the moderate geomagnetic storm during 9 July $L_D(1.5 \leq E \leq 2.7$ keV) was located deep within the outer zone at $L \simeq 4.0$ (cf Figure 6). It is of further interest to note that the maximum intensities of electrons ($1 \lesssim E \lesssim 10$ keV) can be located <u>inside</u> the 'trapping boundary' (Figure 9), <u>outside</u> the 'trapping boundary' (Figure 11), or may <u>straddle</u> this position of the termination of relatively high electron ($E > 45$ keV) intensities (Figure 10) near local midnight in the vicinity of the magnetic equatorial plane.

Simultaneous observations of proton ($3.0 \leq E \leq 4.8$ keV, $12 \leq E \leq 19$ keV, and $31 \leq E \leq 49$ keV) intensities during the inbound pass on 1 July (see Figure 10 for corresponding measurements of electron intensities) are presented in Figure 12. Of primary interest is the occurrence of enhanced intensities of protons ($E \gtrsim 10$ keV) when compared to the intensities of protons $E \lesssim 5$ keV inside the 'trapping boundary' designated by the dashed line at $L = 8.5$. An example of low-energy proton distributions observed during <u>local evening</u> has been given previously by Frank [1967b] and is reproduced here in Figure 13; several useful coordinates for this outbound pass are presented in Figure 14. Note that higher energy protons ($E \gtrsim 3$ keV) have maximum intensities at $L \lesssim 10$ and lower energy protons ($E \lesssim 2$ keV) have

pronounced maximum intensities at $L \gtrsim 10$. This gross feature of the proton distributions is typical of many of the sets of intensity profiles observed in the evening-midnight quadrant of the earth's magnetosphere.

Several of the principal results of our initial survey of the low-energy charged particle distributions within the earth's outer magnetosphere have been summarized above. We note that the observations reported here of generally lower energy electrons and higher energy protons with decreasing radial distance over $5 \lesssim L \lesssim 10$ in the evening-midnight quadrant of the magnetosphere near the equatorial plane are in substantial qualitative agreement with calculations of the adiabatic motion of solar wind electrons and protons in a current model of the geoelectric and geomagnetic fields [Hones, 1963; Taylor and Hones, 1965; Taylor 1966]. Although we are continuing this investigation with a considerably larger body of observations, delineation of a single acceleration mechanism or magnetospheric model is obviated by the present unavailability of simultaneous measurements of electric and magnetic fields.

ACKNOWLEDGEMENTS

This research was supported in part by the National Aeronautics and Space Administration under Grant NsG-233-62 and Contract NAS5-2054 and by the Office of Naval Research under Contract Nonr-1509(06).

REFERENCES

Akasofu, S.-I. and S. Chapman, On the asymmetric development of magnetic storm fields in low and middle latitudes, Planet. Space Sci., 12, 607-626, 1964.

Alfvén, H. and C.-G. Fälthammar, Cosmical electrodynamics, Oxford at the Clarendon Press, 1963.

Axford, W. I. and C. O. Hines, A unifying theory of high-latitude geophysical phenomena and geomagnetic storms, Can. J. Phys., 39, 1433-1464, 1961.

Block, L. P., On the distribution of electric fields in the magnetosphere, J. Geophys. Res., 71, 855-864, 1966.

Cahill, L. J., Jr., Inflation of the inner magnetosphere during a magnetic storm, J. Geophys. Res., 71, 4505-4519, 1966.

Chapman, S. and V. C. A. Ferraro, A new theory of magnetic storms, Terrestrial Magnetism and Atmospheric Electricity, Vol. 36, 77, 171, 1931: Vol. 37, 147, 421, 1932: and Vol. 38, 79, 1933.

Craven, John D., Temporal variations of electron intensities at low altitudes in the outer radiation zone as observed with Satellite Injun 3, J. Geophys. Res., 71, 5643-5663, 1966.

Davis, L. R., Low energy trapped protons and electrons, in Proc. Plasma Space Sci. Symp., ed. by C. C. Chang and S. S. Huang, D. Reidel Publishing Co., Dordrecht-Holland, pp. 212-226, 1965.

Dessler, A. J. and E. N. Parker, Hydromagnetic theory of geomagnetic storms, J. Geophys. Res., 64, 2239-2252, 1959.

Dessler, A. J., W. B. Hanson and E. N. Parker, Formation of the geomagnetic storm main-phase ring current, J. Geophys. Res., 66, 3631-3637, 1961.

Frank, L. A., A survey of electrons E > 40 keV beyond 5 earth radii with Explorer XIV, J. Geophys. Res., 70, 1593-1626, 1965a.

Frank, L. A., Inward radial diffusion of electrons of greater than 1.6 million electron volts in the outer radiation zone, J. Geophys. Res., 70, 3533-3540, 1965b.

Frank, L. A., On the local-time dependence of outer radiation zone electron (E > 1.6 MeV) intensities near the magnetic equator, J. Geophys. Res., 70, 4131-4138, 1965c.

Frank, L. A., Observations of magnetospheric boundary phenomena, in Radiation Trapped in the Earth's Magnetic Field, ed. by B. N. McCormac, D. Reidel Publishing Co., Dordrecht-Holland, pp. 422-446, 1966a.

Frank, L. A., Explorer 12 observations of the temporal variations of low-energy electron intensities in the outer radiation zone during geomagnetic storms, J. Geophys. Res., 71, 4631-4639, 1966b.

Frank, L. A., Initial observations of low-energy electrons in the earth's magnetosphere with OGO 3, J. Geophys. Res., 72, 185-195, 1967a.

Frank, L. A., Several observations of low-energy protons and electrons in the earth's magnetosphere with OGO 3, J. Geophys. Res., 72, 1905-1916, 1967b.

Frank, L. A., On the extraterrestrial ring current during geomagnetic storms, J. Geophys. Res., (accepted for publication), 1967c.

Frank, L. A. and R. L. Swisher, On the energy fluxes of low-energy protons and positive ions in the earth's inner radiation zone, J. Geophys. Res., (submitted for publication), 1967.

Frank, L. A. and J. A. Van Allen, A survey of magnetospheric boundary phenomena, Research in Geophysics, Vol. 1: Sun, Upper Atmosphere, and Space, Chapter 7, pp. 161-187, ed. by Hugh Odishaw, M.I.T. Press, 1964.

Frank, L. A., J. A. Van Allen, and H. K. Hills, A study of charged particles in the earth's outer radiation zone with Explorer 14, J. Geophys. Res., 69, 2171-2191, 1964.

Freden, S. C., J. B. Blake, and G. A. Paulikas, Spatial variation of the inner zone trapped proton spectrum, J. Geophys. Res., 70, 3113-3116, 1965.

Freeman, John W., Detection of an intense flux of low-energy protons or ions trapped in the inner radiation zone, J. Geophys. Res., 67, 921-928, 1962.

Gabbe, J. D. and W. L. Brown, Some observations of the distributions of energetic protons in the earth's radiation belts between

1962 and 1964, in Radiation Trapped in the Earth's Magnetic Field, Ed. by B. M. McCormac, D. Reidel Publishing Co., Dordrecht-Holland, pp. 165-184, 1966.

Hess, W. N., The earth's radiation belt, in Introduction to Space Science, Chapter 4, 165-203, Ed. by W. N. Hess, Gordon and Breach, 1965.

Hones, E. W., Jr., Motions of charged particles trapped in the earth's magnetosphere, J. Geophys. Res., 68, 1209-1219, 1963.

Jensen, D. C. and J. C. Cain, An interim geomagnetic field (abstract), J. Geophys. Res., 67, 3568-3569, 1962.

Kennel, C. F. and H. E. Petschek, "Van Allen belt plasma physics", Avco Everett Res. Rep., 259, 1966.

Liemohn, H., The lifetime of radiation belt protons with energies between 1 keV and 1 MeV, J. Geophys. Res., 66, 3593-3595, 1961.

Lincoln, J. Virginia, Geomagnetic and solar data, J. Geophys. Res., 71, 5211, 5784, 1966.

McIlwain, C. E., The radiation belts, natural and artificial, Science, 142, No. 3590, 355-361, 1963.

McIlwain, C. E., Ring current effects on trapped particles, J. Geophys. Res., 71, 3623-3628, 1966.

O'Brien, B. J., The trapped-radiation zones, Space Physics, ed. Le Galley and Rosen, 505-572, John Wiley and Sons, New York, 1964a.

O'Brien, B. J., High-latitude geophysical studies with satellite Injun 3. 3. Precipitation of electrons into the atmosphere, J. Geophys. Res., 69, 13-43, 1964b.

Owens, H. D. and L. A. Frank, Electron omnidirectional intensity contours in the earth's outer radiation zone at the magnetic equator, J. Geophys. Res., (to be submitted for publication), 1967.

Sckopke, N., A general relation between the energy of trapped particles and the disturbance field near the earth, J. Geophys. Res., 71, 3125-3130, 1966.

Shabansky, V. P., Radiation belts (a review), Geomagnetism and Aeronomy, 5, 765-789, 1965.

Taylor, Harold E., Adiabatic motion of outer-zone particles in a model of the geoelectric and geomagnetic fields, J. Geophys. Res., 71, 5135-5147, 1966.

Taylor, H. E. and E. W. Hones, Jr., Adiabatic motion of auroral particles in a model of the electric and magnetic field surrounding the earth, J. Geophys. Res., 70, 3605-3628, 1965.

Van Allen, J. A., Dynamics, composition, and origin of geomagnetically trapped radiation, Space Science, 226-274, ed. by D. P. Le Galley, John Wiley and Sons, Inc., New York, 1963.

Vette, James I., Models of the Trapped Radiation Environment, Vol. I: Inner zone protons and electrons, NASA SP-3024, 1966.

FIGURE CAPTIONS

Figure 1. Contours of constant omnidirectional intensities of electrons ($E \geq 40$ keV, $E \geq 230$ keV and $E \geq 1.6$ MeV) in the outer radiation zone at the magnetic equator observed with an array of G.M. tubes borne on Explorer 14 during October through November 1962. Daily sum K_p, ΣK_p, is also shown in order to indicate periods of relative geomagnetic activity (after Owens and Frank [1967]).

Figure 2. Continuation of Figure 1 for the period December 1962 through January 1963 (after Owens and Frank [1967]).

Figure 3. Comparison of Injun 1 observations of large energy fluxes of protons or ions (500 eV $\lesssim E \lesssim$ 1 MeV) [Freeman, 1962] and OGO 3 measurements of the upper limits for energy fluxes of positive ions ($100 \leq \frac{E}{Q} \leq 50$ keV) in the earth's inner radiation zone (after Frank and Swisher [1967]).

Figure 4. Hourly $D_{ST}(H)$ values for the period covering the geomagnetic storm during early July 1966 (after Frank [1967c]).

Figure 5. Directional intensities of protons ($31 \leq E \leq 49$ keV) as functions of L at low magnetic latitudes during the pre-storm, main phase, recovery phase and post-storm periods of the early-July geomagnetic storm (after Frank [1967c]).

Figure 6. Electron (200 eV $\leq$ E $\leq$ 50 keV) and proton (200 eV $\leq$ E $\leq$ 50 keV) energy densities as functions of L at low magnetic latitudes during the main phase of the early-July storm (after Frank [1967c]).

Figure 7. Contours of constant proton (200 eV $\leq$ E $\leq$ 50 keV) energy densities in a R-λ_m coordinate system on 9 July 1966 (after Frank [1967c]).

Figure 8. Directional intensities of electrons (630 $\leq$ E $\leq$ 1100 eV, 1.5 $\leq$ E $\leq$ 2.7 keV, 6.8 $\leq$ E $\leq$ 12 keV, 27 $\leq$ E $\leq$ 47 keV and E > 45 keV) observed during an inbound pass through the outer magnetosphere near the midnight meridional plane on 22-23 June 1966. Several useful coordinates for these observations are included (see text).

Figure 9. Continuation of Figure 8 for directional intensities of electrons (1.5 $\leq$ E $\leq$ 2.7 keV, 3.8 $\leq$ E $\leq$ 6.8 keV, 14 $\leq$ E $\leq$ 24 keV, and E > 45 keV) on 27 June 1966.

Figure 10. Continuation of Figure 9 for 1 July.

Figure 11. Continuation of Figure 9 for 3 July.

Figure 12. Simultaneous observations of directional intensities of protons (3.0 $\leq$ E $\leq$ 4.8 keV, 12 $\leq$ E $\leq$ 19 keV, and 31 $\leq$ E $\leq$ 49 keV) as functions of shell-parameter L for the inbound pass on 1 July. The measurements are obtained at identical pitch angles and simultaneously with the observations of low-energy electron intensities displayed in Figure 10.

Figure 13. Directional intensities of protons within six energy bandpasses as functions of L for an outbound pass near the evening meridional plane on 11 June 1966 (after Frank [1967b]).

Figure 14. Several useful coordinates for the satellite position during the series of observations displayed in Figure 13: geomagnetic latitude, λ_m; solar magnetospheric latitude, θ_{SM}; solar ecliptic latitude and longitude, θ_{SE} and φ_{SE} (after Frank [1967b]).

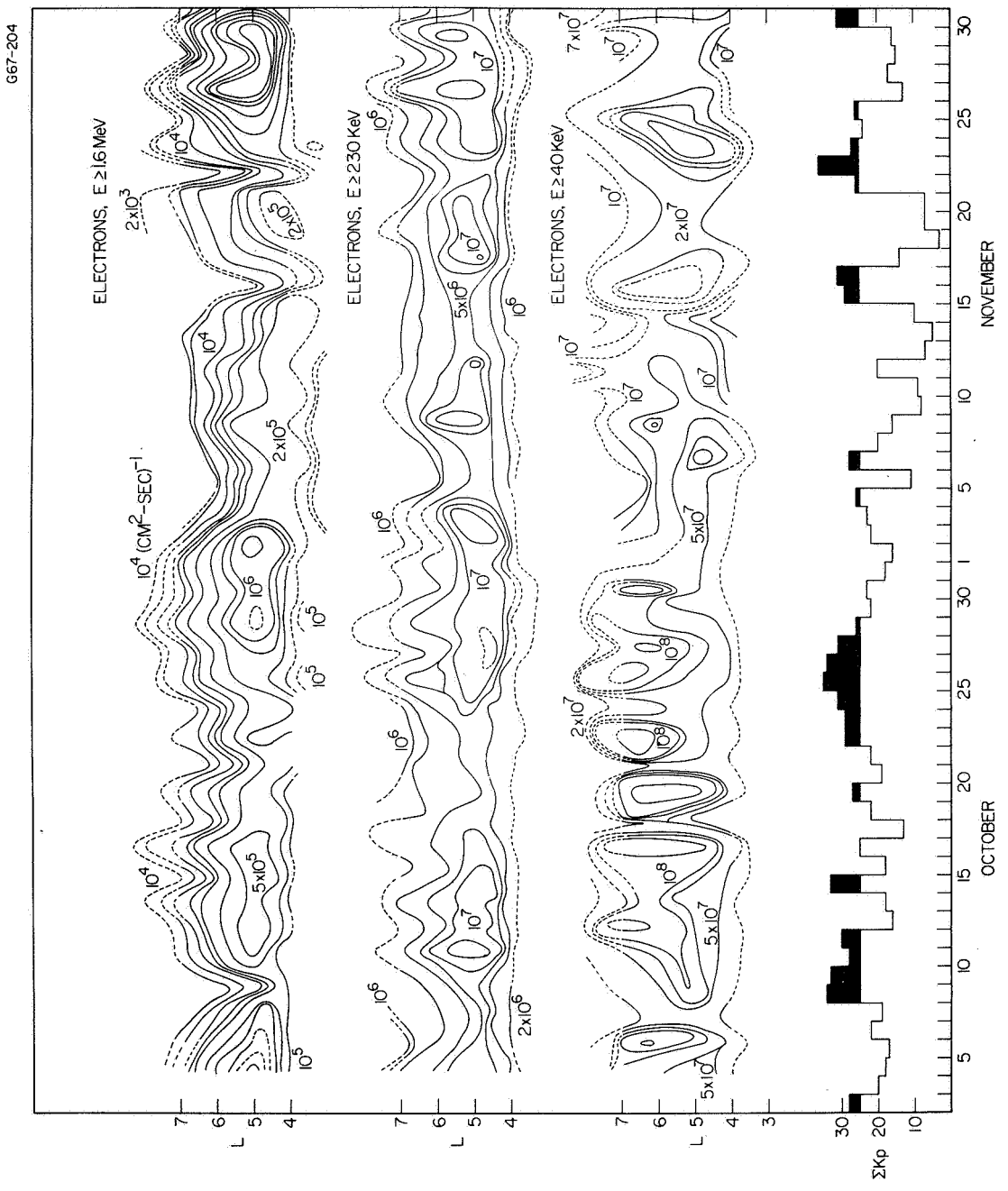
G67-204
ELECTRONS, E ≥ 1.6 MeV
10^4 (CM^2-SEC)$^{-1}$
ELECTRONS, E ≥ 230 KeV
ELECTRONS, E ≥ 40 KeV
L
ΣKp
OCTOBER
NOVEMBER

Figure 1

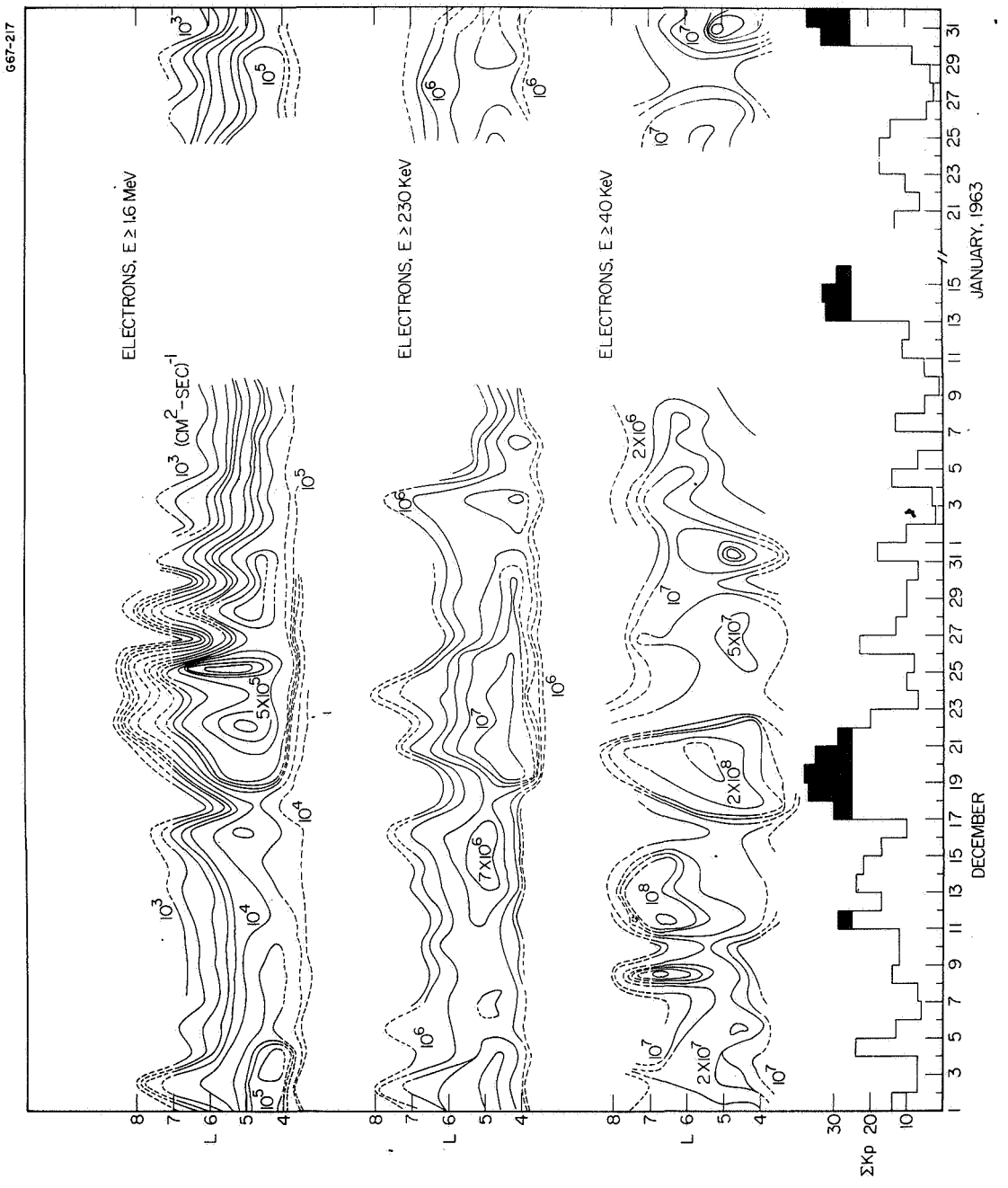
667-217
ELECTRONS, E ≥ 1.6 MeV
ELECTRONS, E ≥ 230 KeV
ELECTRONS, E ≥ 40 KeV
10^3 (CM^2-SEC)$^{-1}$
L
ΣKp
DECEMBER
JANUARY, 1963

Figure 2

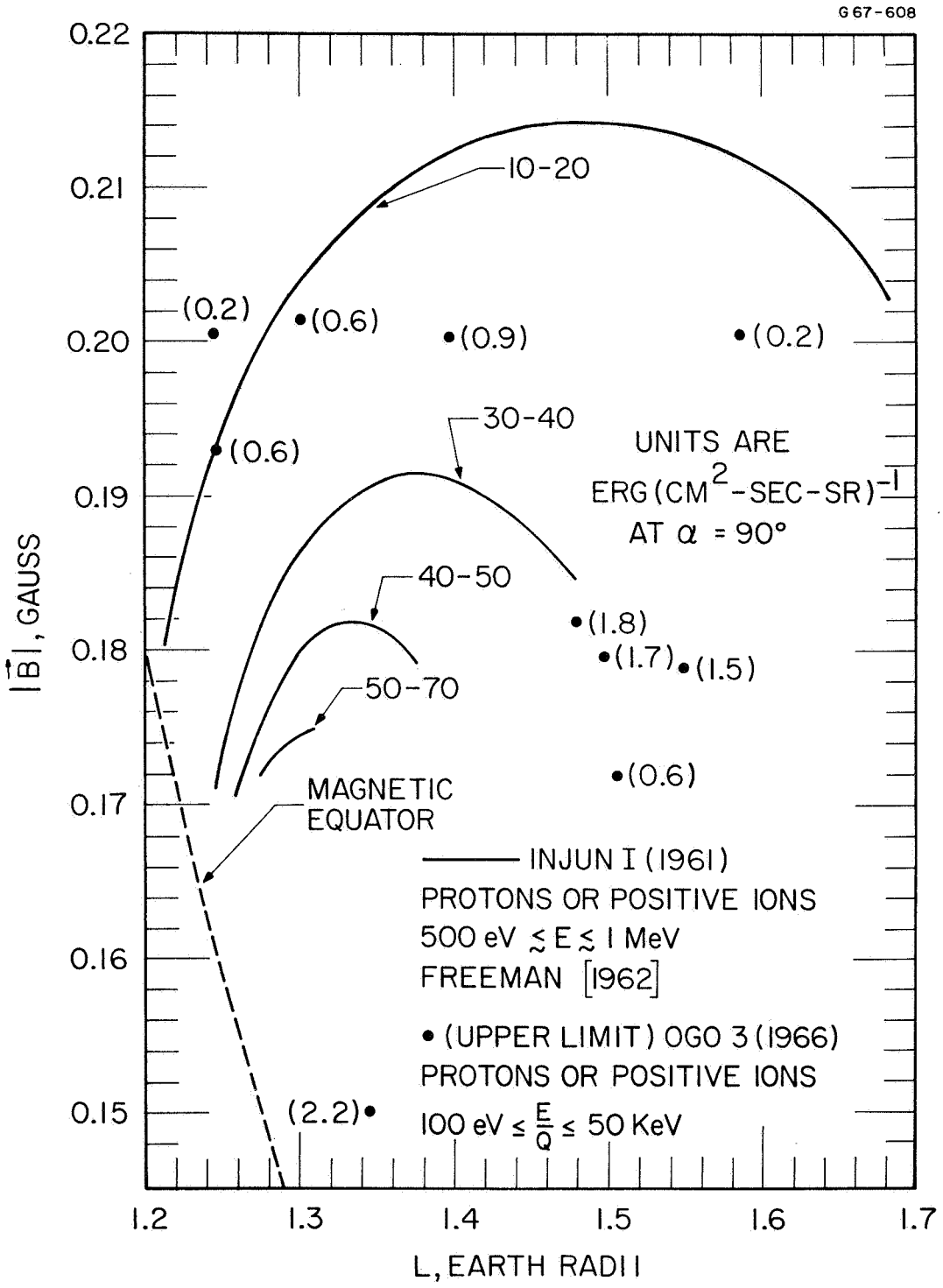
G 67-608
0.22
0.21
0.20
0.19
0.18
0.17
0.16
0.15
|B|, GAUSS
10-20
30-40
40-50
50-70
(0.2)
(0.6)
(0.9)
(0.2)
(0.6)
(1.8)
(1.7)
(1.5)
(0.6)
(2.2)
UNITS ARE
ERG (CM^2-SEC-SR)$^{-1}$
AT α = 90°
MAGNETIC
EQUATOR
INJUN I (1961)
PROTONS OR POSITIVE IONS
500 eV $\lesssim$ E $\lesssim$ 1 MeV
FREEMAN [1962]
• (UPPER LIMIT) OGO 3 (1966)
PROTONS OR POSITIVE IONS
100 eV $\leq \frac{E}{Q} \leq$ 50 KeV
1.2
1.3
1.4
1.5
1.6
1.7
L, EARTH RADII

Figure 3

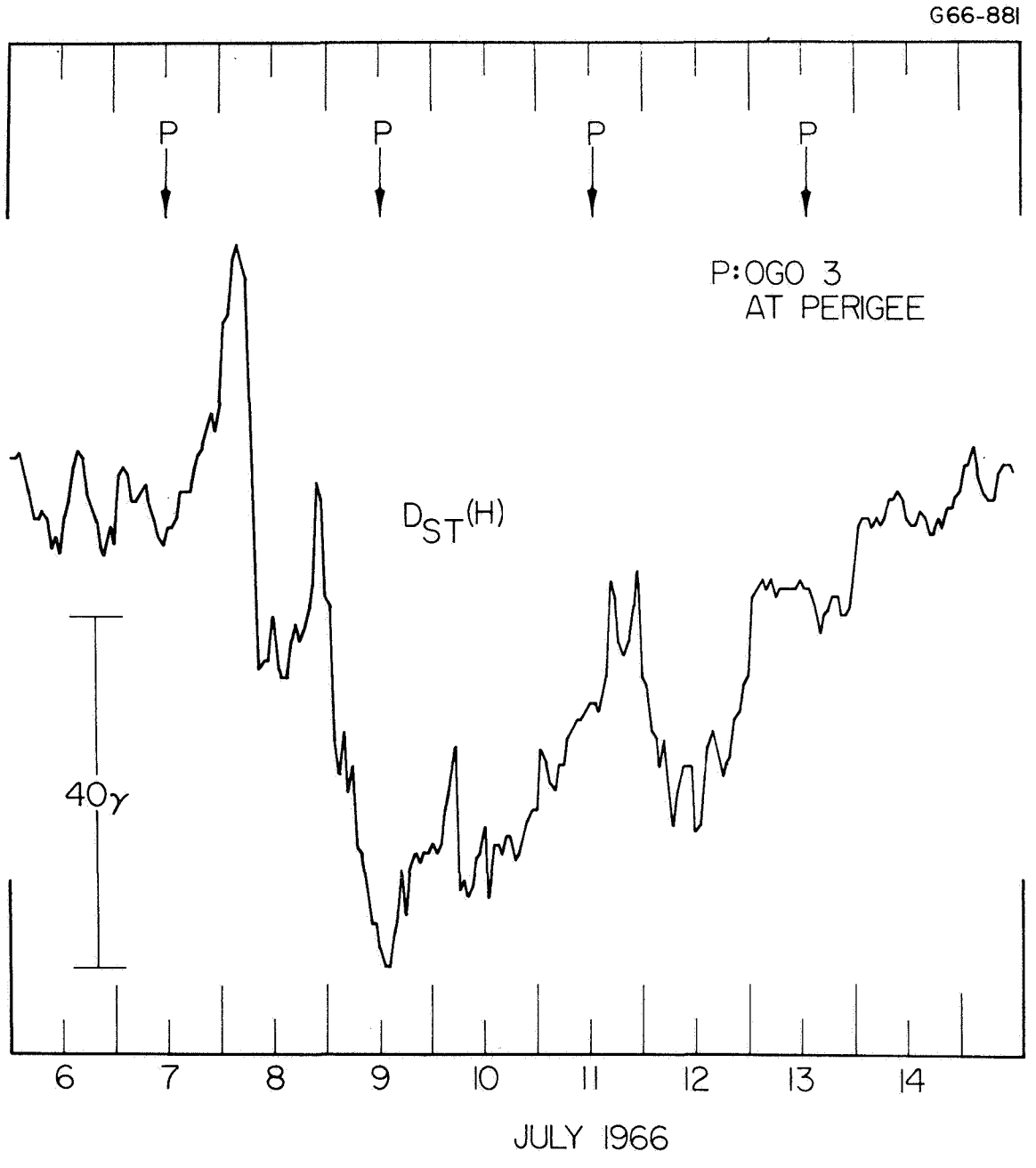
G66-881
P
P
P
P
P:OGO 3
AT PERIGEE
D_{ST}(H)
40γ
6
7
8
9
10
11
12
13
14
JULY 1966

Figure 4

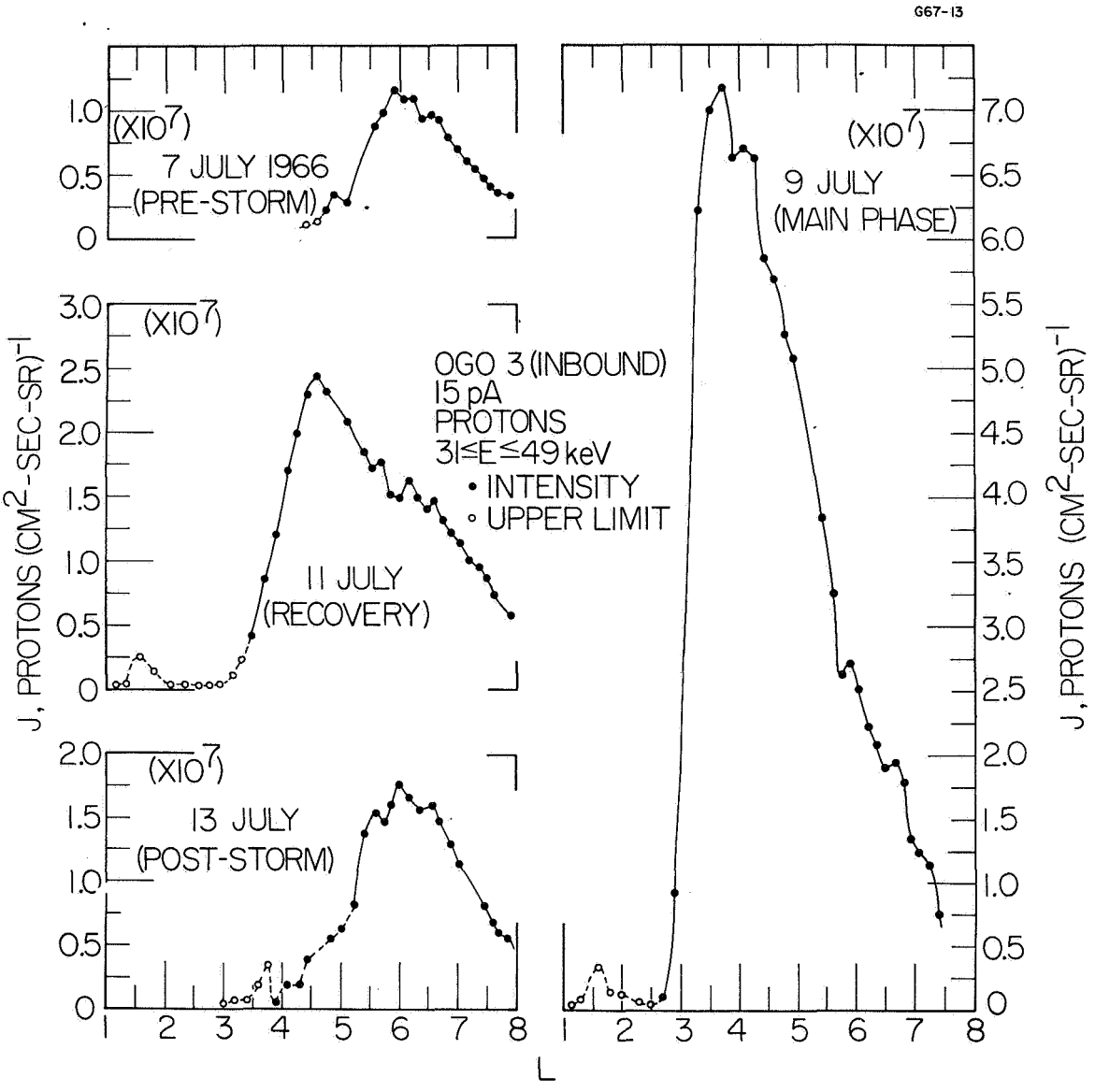
G67-13
(X10^7)
7 JULY 1966
(PRE-STORM)
(X10^7)
11 JULY
(RECOVERY)
OGO 3 (INBOUND)
15 pA
PROTONS
31≤E≤49 keV
• INTENSITY
◦ UPPER LIMIT
(X10^7)
13 JULY
(POST-STORM)
(X10^7)
9 JULY
(MAIN PHASE)
J, PROTONS (CM^2-SEC-SR)^-1
J, PROTONS (CM^2-SEC-SR)^-1
L

Figure 5

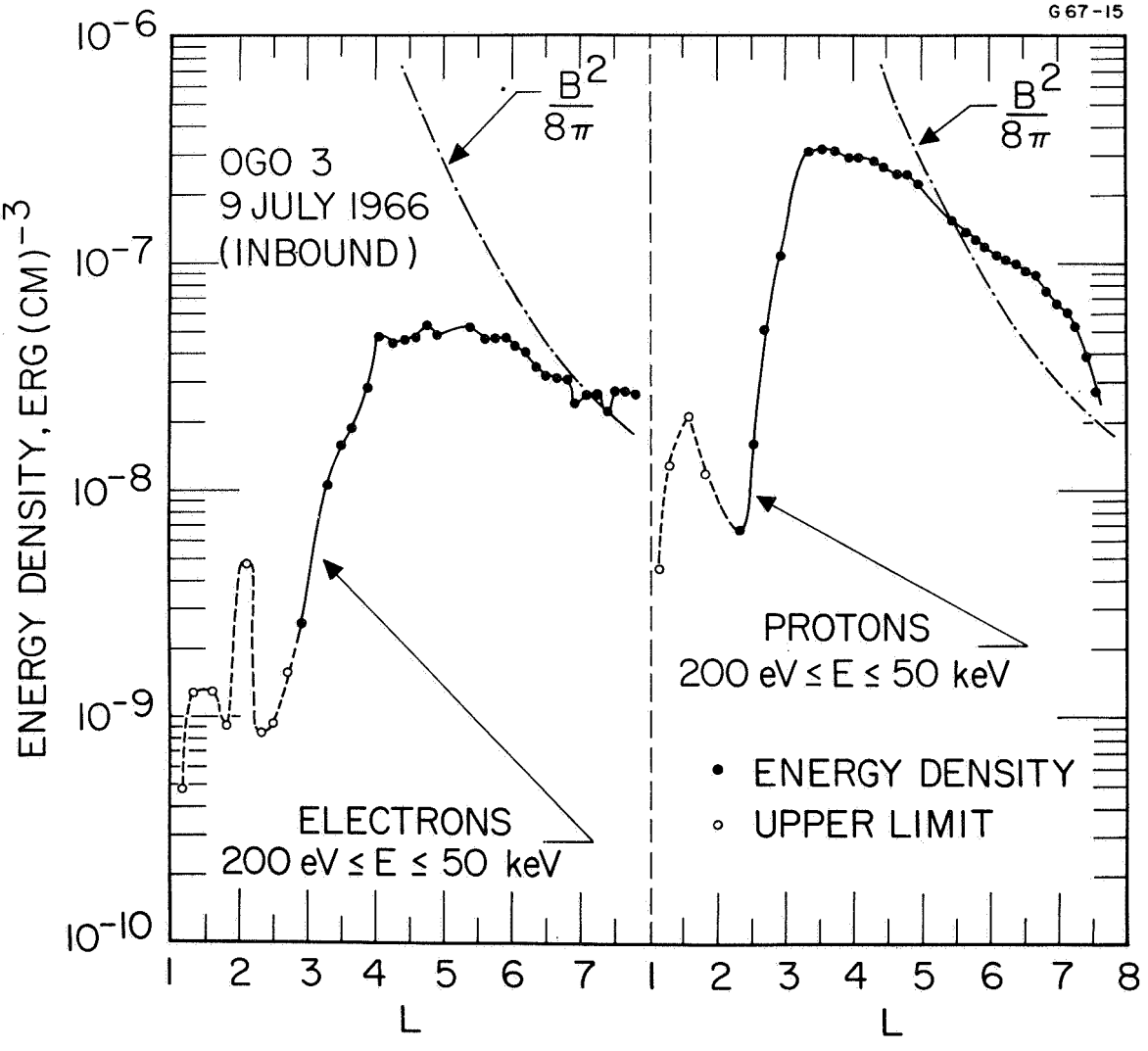
G 67-15
ENERGY DENSITY, ERG (CM)$^{-3}$
10^{-6}
10^{-7}
10^{-8}
10^{-9}
10^{-10}
$\frac{B^2}{8\pi}$
OGO 3
9 JULY 1966
(INBOUND)
ELECTRONS
200 eV ≤ E ≤ 50 keV
PROTONS
200 eV ≤ E ≤ 50 keV
• ENERGY DENSITY
◦ UPPER LIMIT
1 2 3 4 5 6 7
L
1 2 3 4 5 6 7 8
L

Figure 6

G67-76

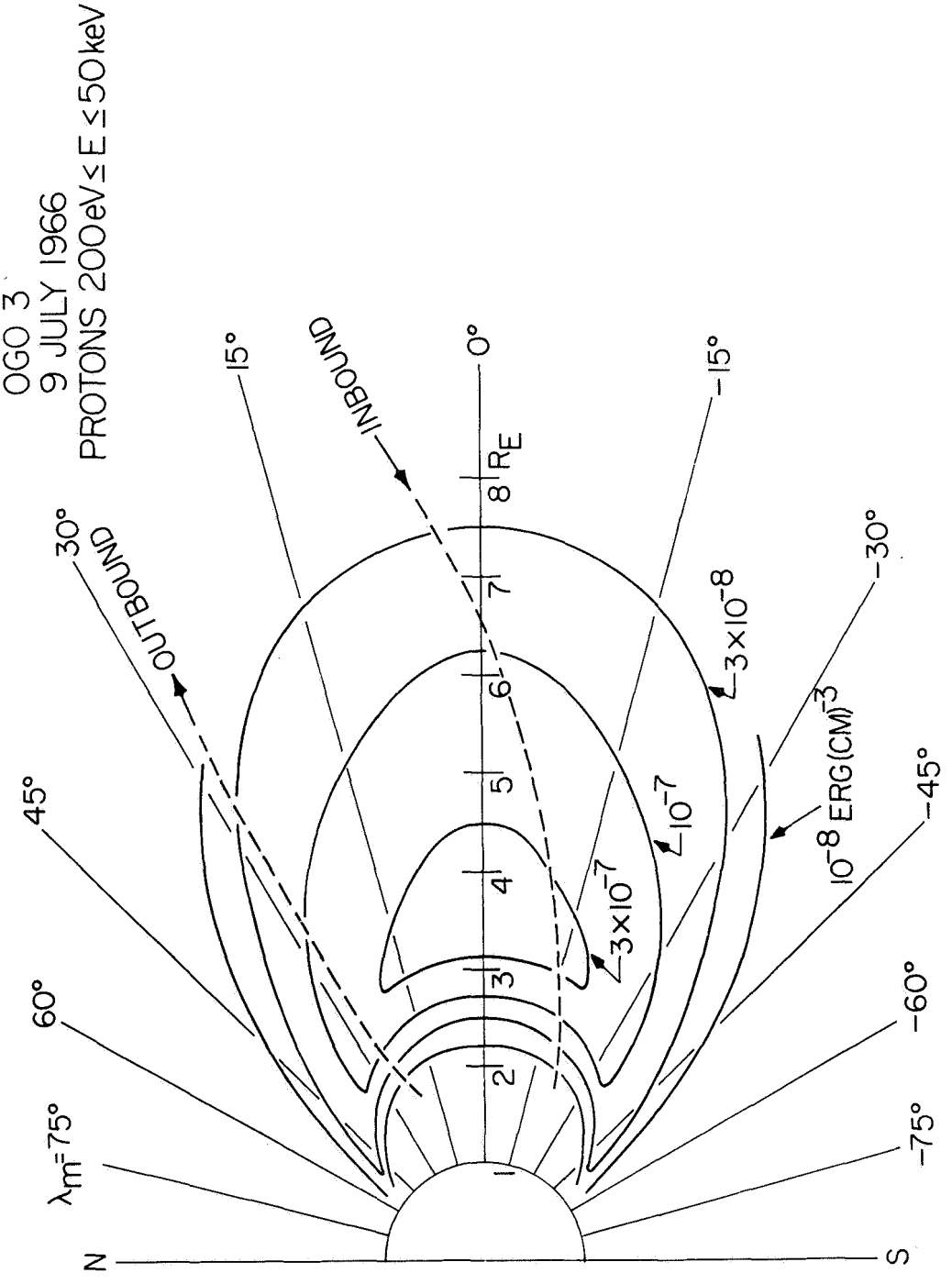

Figure 7

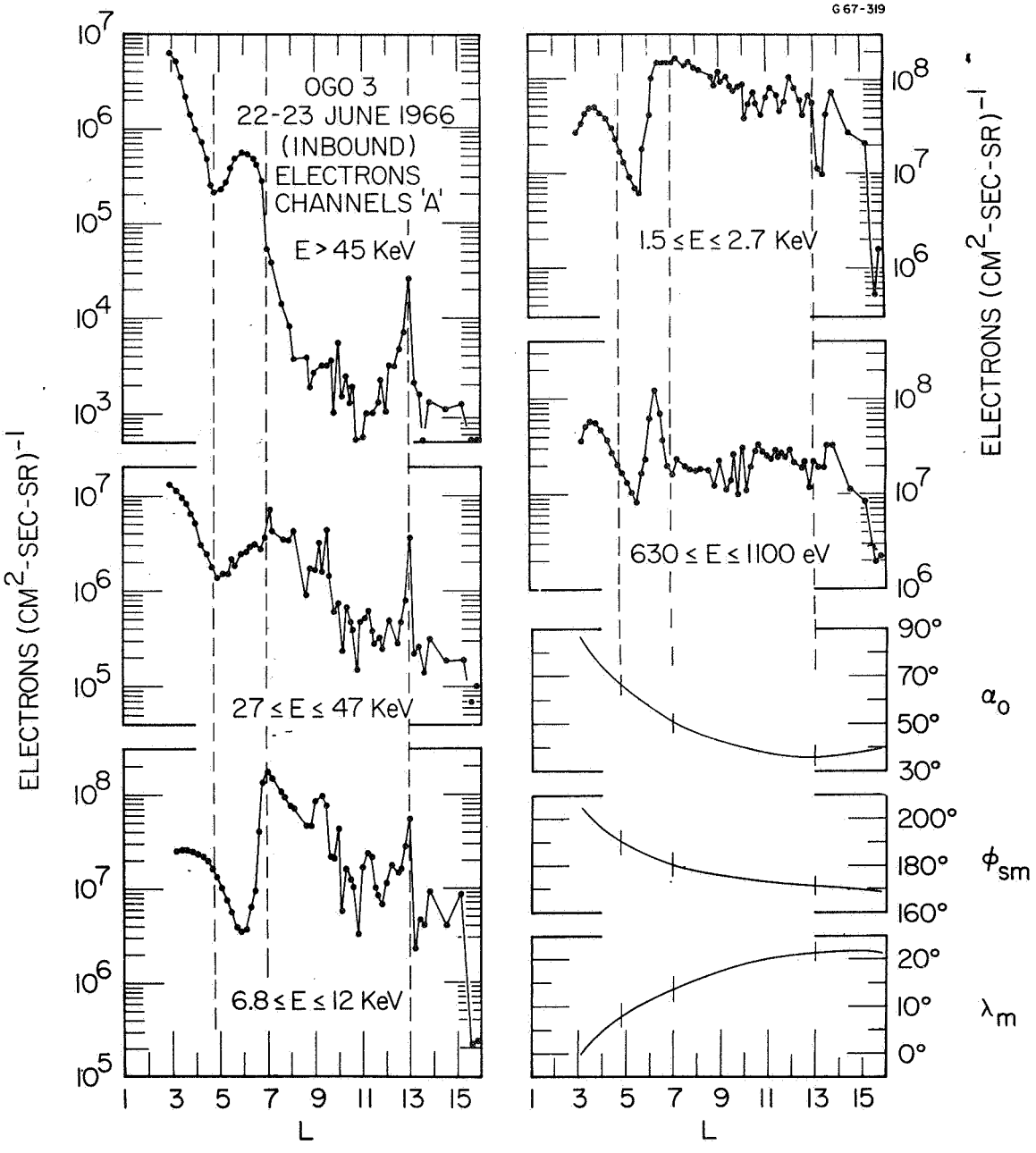
G67-319
OGO 3
22-23 JUNE 1966
(INBOUND)
ELECTRONS
CHANNELS 'A'
E > 45 KeV
27 ≤ E ≤ 47 KeV
6.8 ≤ E ≤ 12 KeV
1.5 ≤ E ≤ 2.7 KeV
630 ≤ E ≤ 1100 eV
ELECTRONS (CM²-SEC-SR)⁻¹
L
α_o
ϕ_{sm}
λ_m

Figure 8

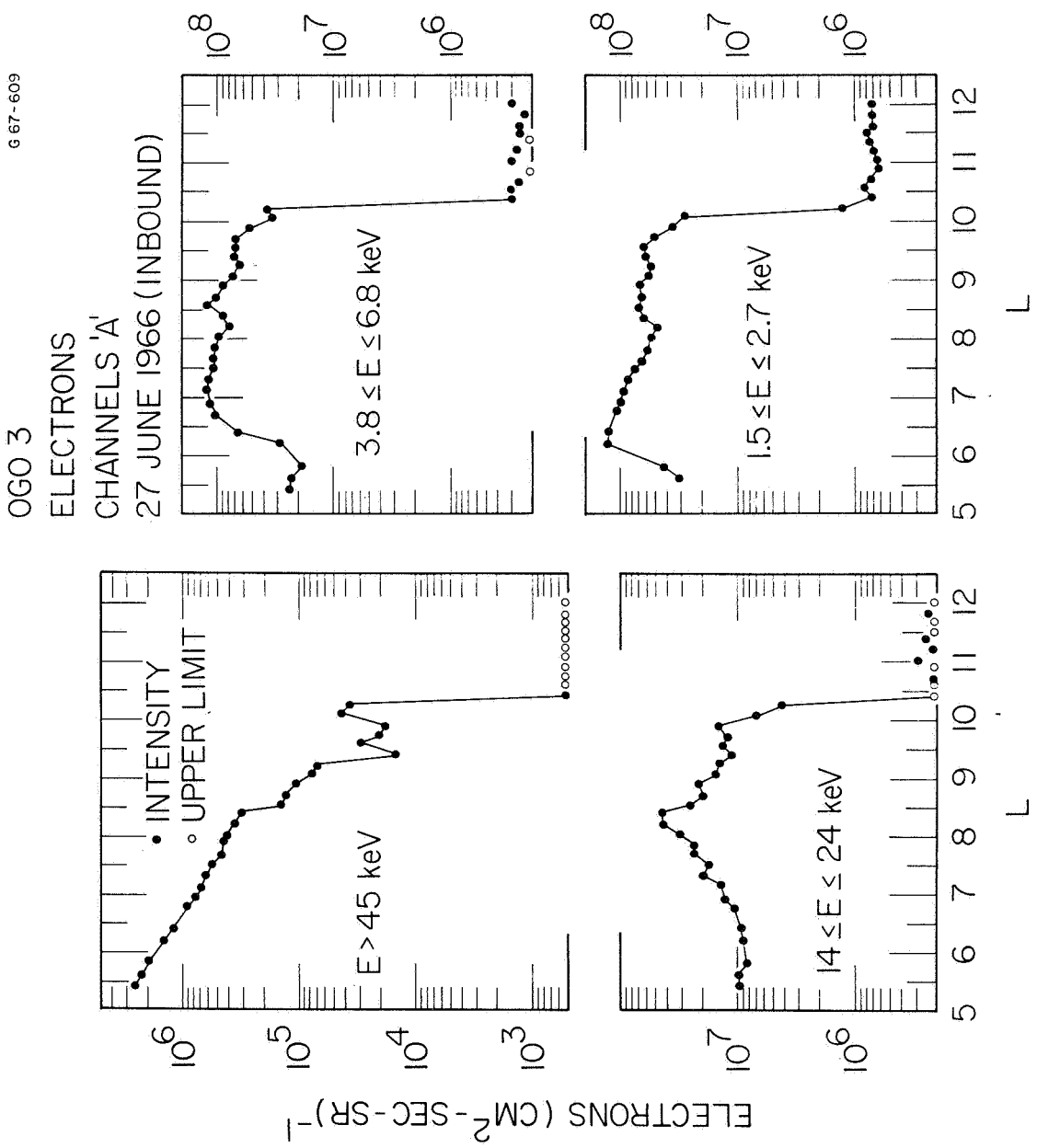
G 67-609
OGO 3
ELECTRONS
CHANNELS 'A'
27 JUNE 1966 (INBOUND)
• INTENSITY
° UPPER LIMIT
E > 45 keV
3.8 ≤ E ≤ 6.8 keV
1.5 ≤ E ≤ 2.7 keV
14 ≤ E ≤ 24 keV
ELECTRONS (CM²-SEC-SR)⁻¹
L

Figure 9

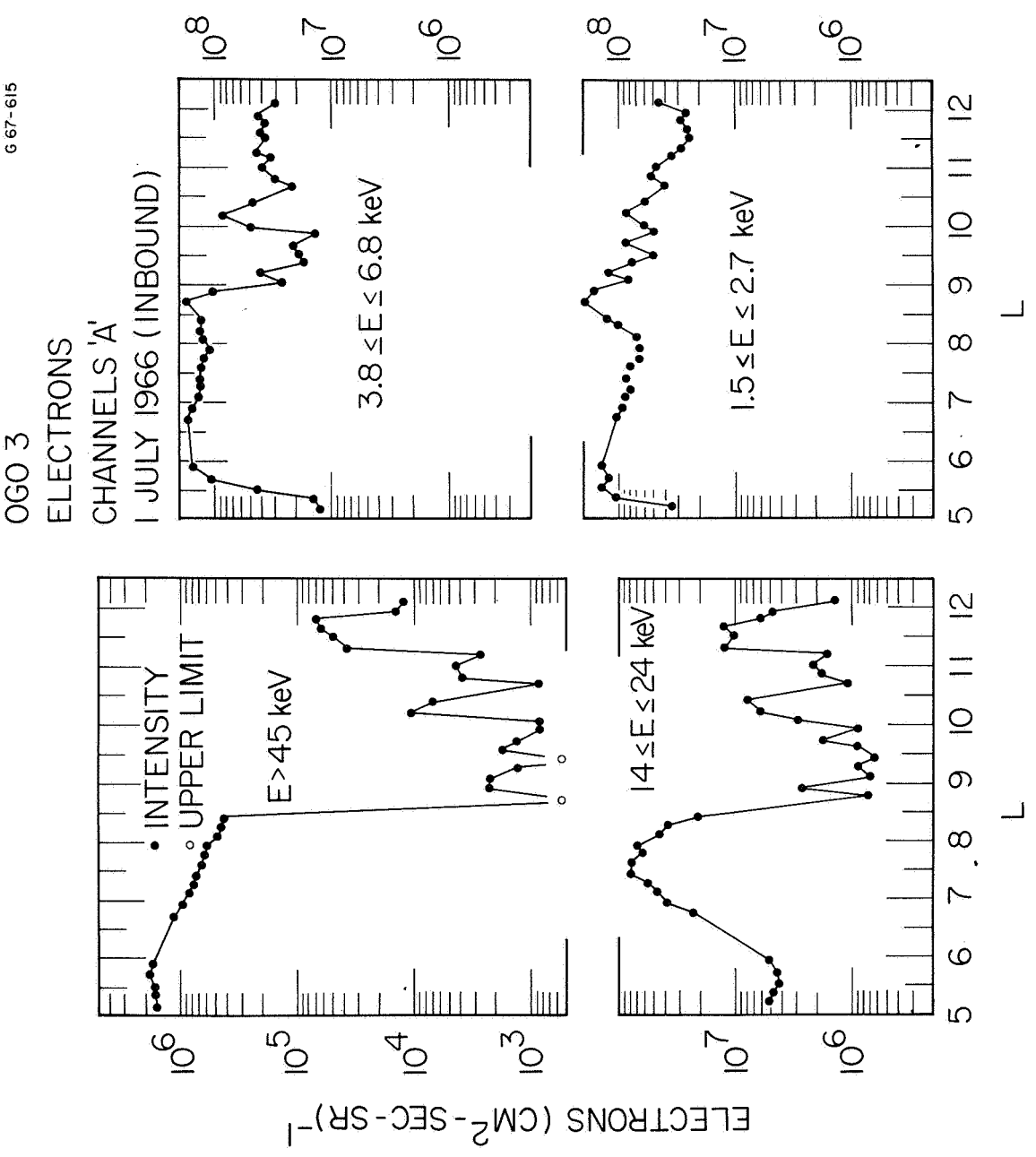
G 67-615
OGO 3
ELECTRONS
CHANNELS 'A'
1 JULY 1966 (INBOUND)
• INTENSITY
° UPPER LIMIT
E>45 keV
3.8 ≤ E ≤ 6.8 keV
1.5 ≤ E ≤ 2.7 keV
14 ≤ E ≤ 24 keV
ELECTRONS (CM²-SEC-SR)⁻¹
L

Figure 10

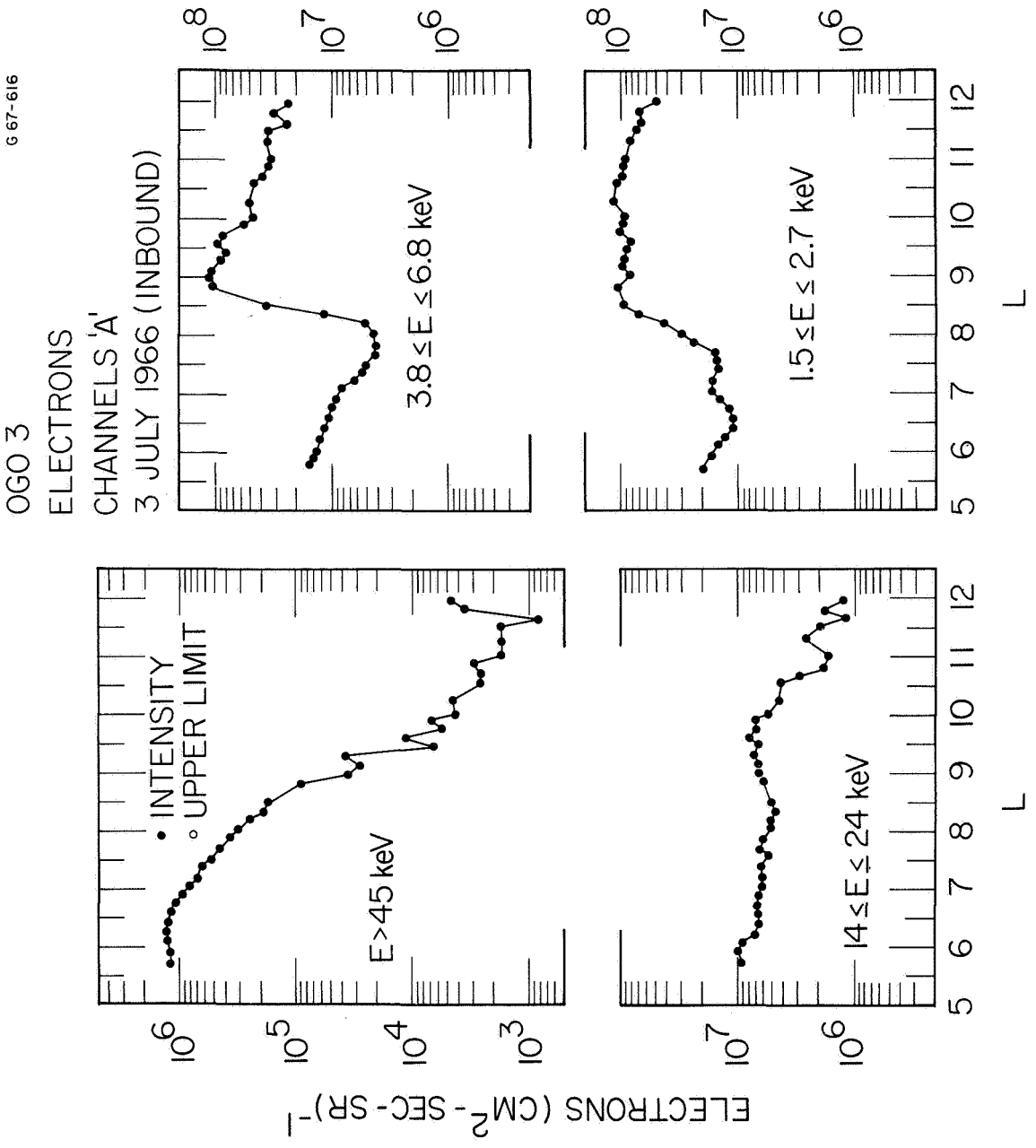
G 67-616
OGO 3
ELECTRONS
CHANNELS 'A'
3 JULY 1966 (INBOUND)
• INTENSITY
° UPPER LIMIT
E>45 keV
3.8≤E≤6.8 keV
1.5≤E≤2.7 keV
14≤E≤24 keV
ELECTRONS (CM²-SEC-SR)⁻¹
L

Figure 11

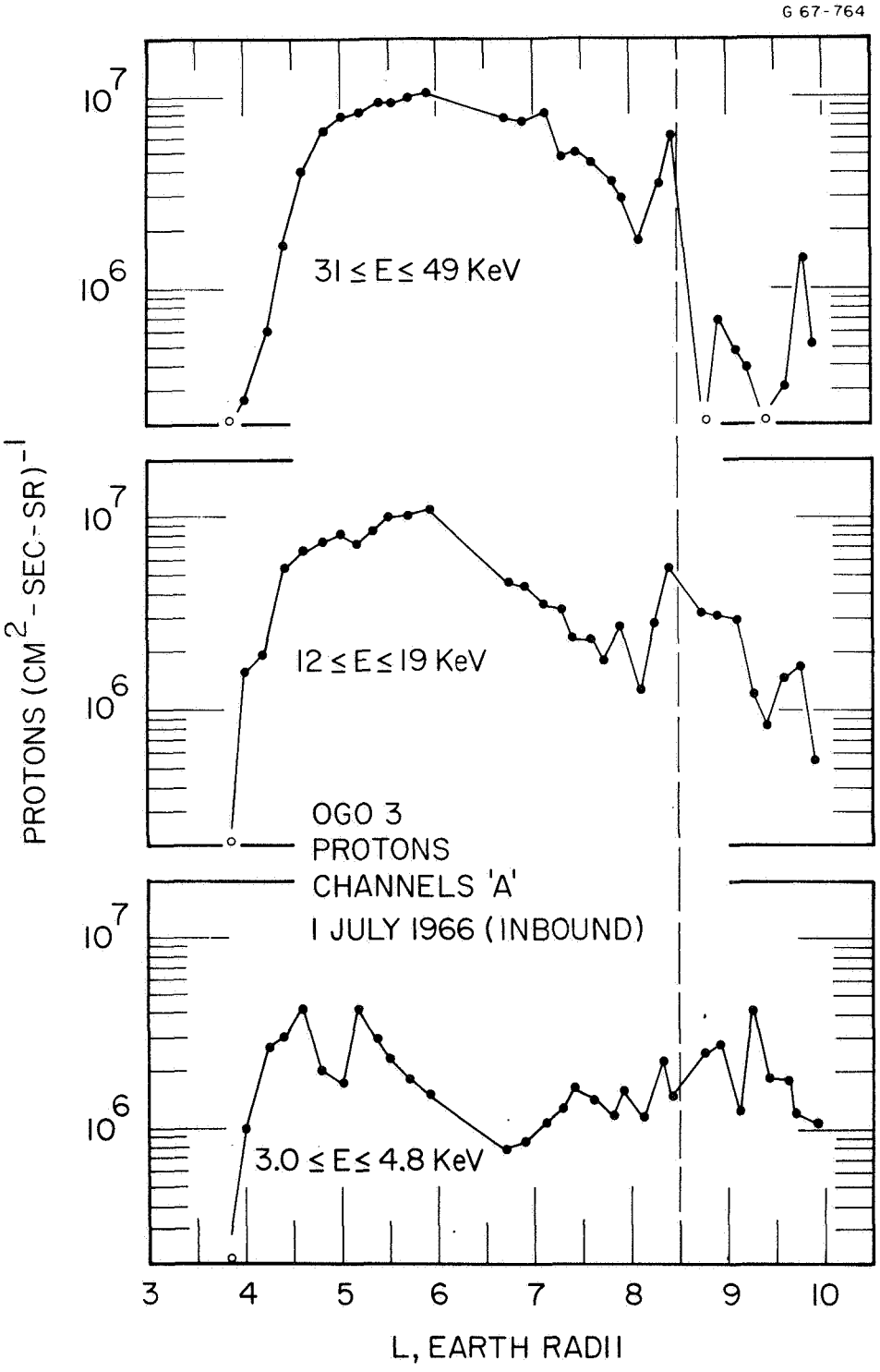
G 67-764
10^7
10^6
31 ≤ E ≤ 49 KeV
12 ≤ E ≤ 19 KeV
3.0 ≤ E ≤ 4.8 KeV
OGO 3
PROTONS
CHANNELS 'A'
1 JULY 1966 (INBOUND)
PROTONS (CM^2-SEC-SR)$^{-1}$
3
4
5
6
7
8
9
10
L, EARTH RADII

Figure 12

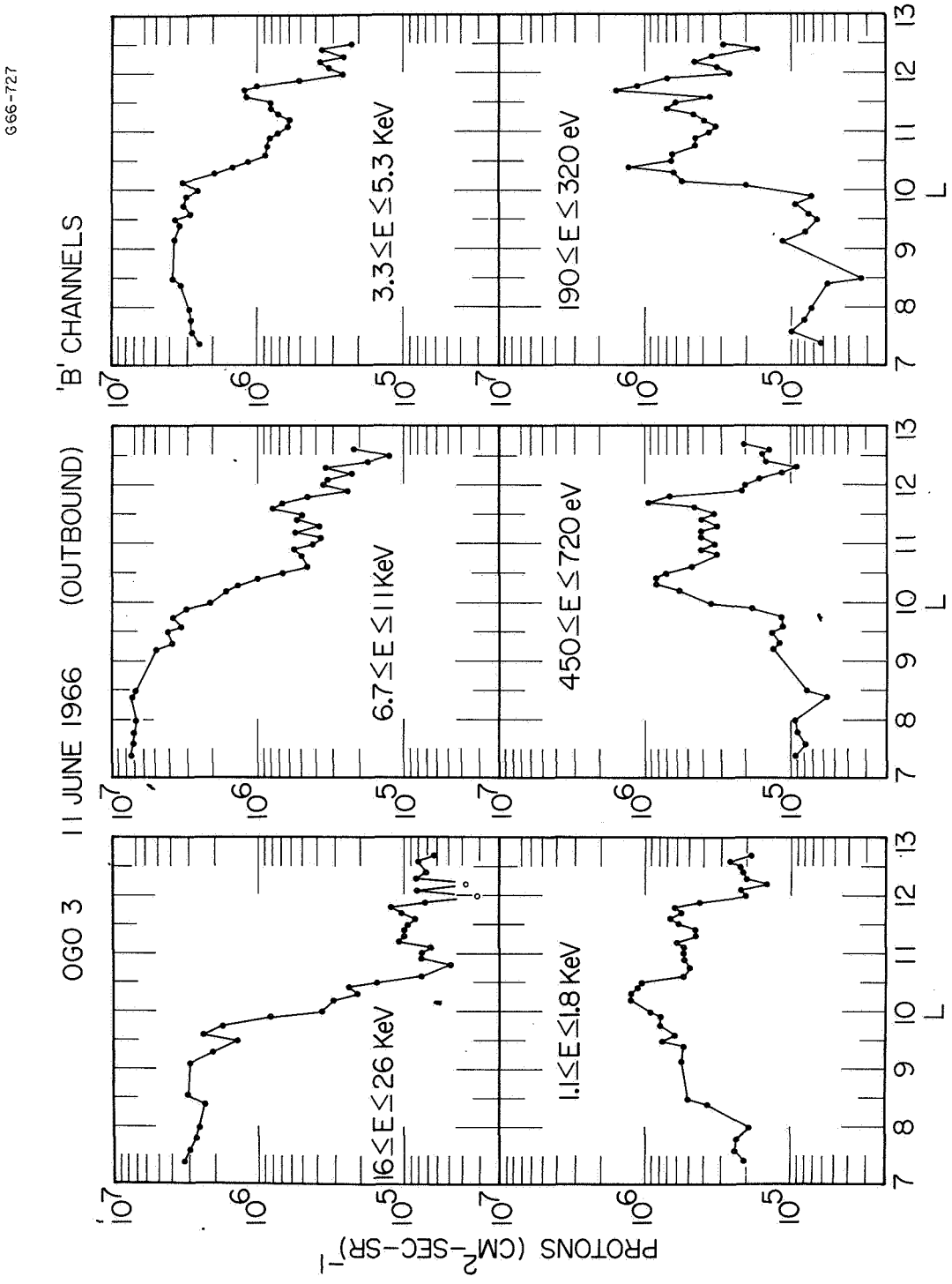
G66-727
OGO 3 11 JUNE 1966 (OUTBOUND) 'B' CHANNELS
PROTONS (CM²-SEC-SR)⁻¹
16≤E≤26 KeV
1.1≤E≤1.8 KeV
6.7≤E≤11KeV
450≤E≤720 eV
3.3≤E≤5.3 KeV
190≤E≤320 eV
L

Figure 13

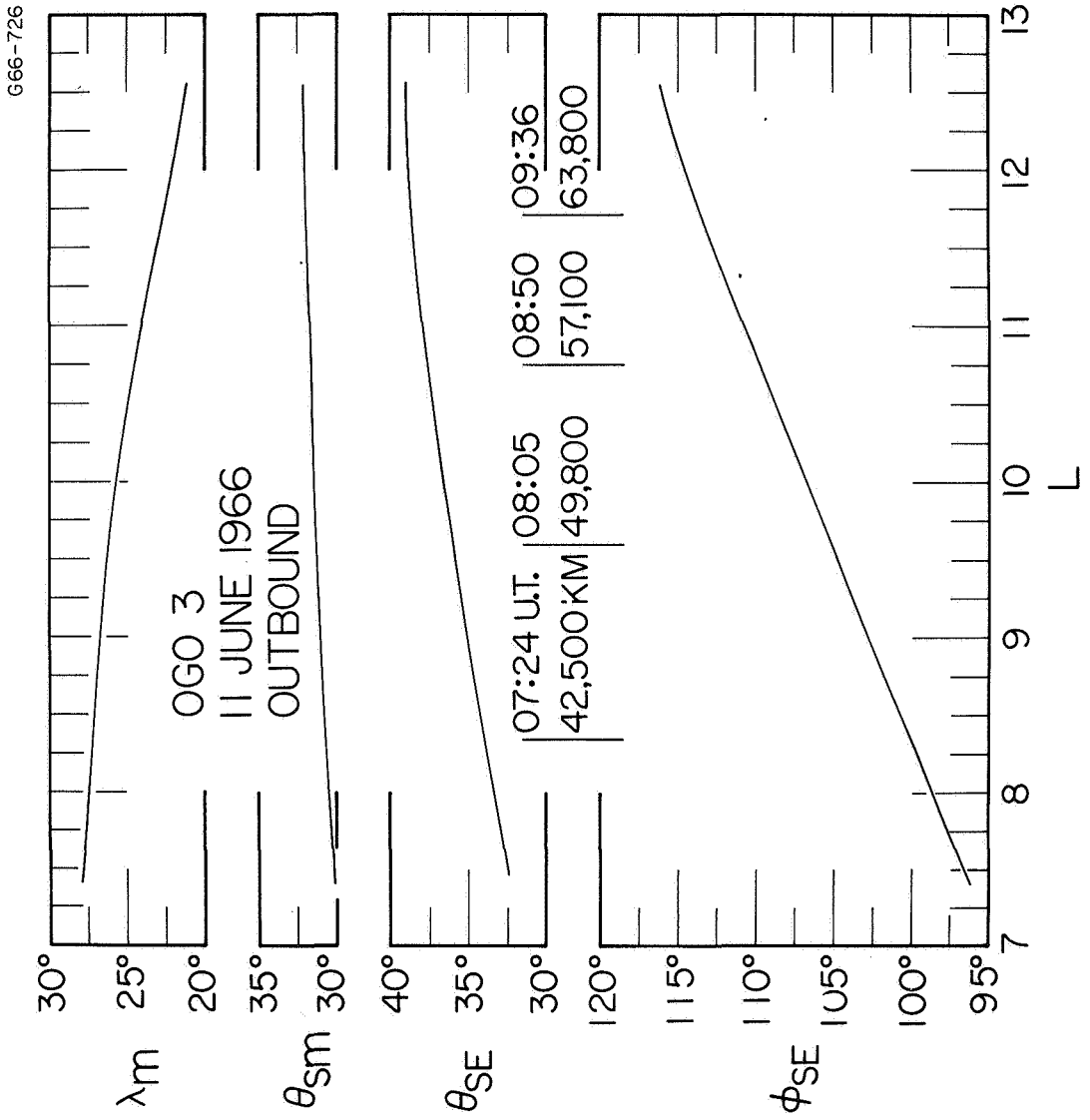
G66-726
OGO 3
11 JUNE 1966
OUTBOUND
07:24 U.T.
42,500 KM
08:05
49,800
08:50
57,100
09:36
63,800
λm
θsm
θSE
φSE
L
30°
25°
20°
35°
30°
40°
35°
30°
120°
115°
110°
105°
100°
95°
7
8
9
10
11
12
13

Figure 14

UNCLASSIFIED

Security Classification

DOCUMENT CONTROL DATA - R&D

(Security classification of title, body of abstract and indexing annotation must be entered when the overall report is classified)

1. ORIGINATING ACTIVITY *(Corporate author)*

University of Iowa
Department of Physics and Astronomy

2a. REPORT SECURITY CLASSIFICATION

UNCLASSIFIED

2b GROUP

3. REPORT TITLE

Recent Observations Of Low-Energy Charged Particles In The Earth's Magnetosphere.

4. DESCRIPTIVE NOTES *(Type of report and inclusive dates)*

Progress July 1967

5. AUTHOR(S) *(Last name, first name, initial)*

FRANK, L. A.

6. REPORT DATE	7a. TOTAL NO. OF PAGES	7b. NO. OF REFS
July 1967	48	41

8a. CONTRACT OR GRANT NO.	9a. ORIGINATOR'S REPORT NUMBER(S)
NONr-1509(06)	U. of Iowa 67-36
b. PROJECT NO.	
c.	9b. OTHER REPORT NO(S) *(Any other numbers that may be assigned this report)*
d.	

10. AVAILABILITY/LIMITATION NOTICES

Distribution of this document is unlimited.

11. SUPPLEMENTARY NOTES	12. SPONSORING MILITARY ACTIVITY
	Office of Naval Research

13. ABSTRACT

Several recent observations of low-energy proton and electron intensities within the energy range ~ 100 eV to 50 keV in the earth's radiation zones with a sensitive array of electrostatic analyzers borne on the earth-satellite OGO 3 during mid-1966 are summarized. Measurements of charged particles of the extraterrestrial ring current during a moderate geomagnetic storm, of the low-energy proton and electron distributions in the vicinity of the midnight 'trapping boundary' near the magnetic equatorial plane, and of upper limits for proton and ion (100 eV $\leq \frac{E}{Q} \leq$ 50 keV) energy fluxes deep within the inner radiation zone are presented together with several introductory comments concerning the morphology of the omnidirectional intensities of energetic electrons ($E \geq$ 40 keV, $\geq$ 230 keV and $\geq$ 1.6 MeV) at the magnetic equator in the outer radiation zone.

DD FORM 1 JAN 64 1473

UNCLASSIFIED

Security Classification

14. KEY WORDS	LINK A		LINK B		LINK C	
	ROLE	WT	ROLE	WT	ROLE	WT
Geomagnetic Storm						
Inner Radiation Zone						
Outer Radiation Zone						
Magnetosphere						

INSTRUCTIONS

1. ORIGINATING ACTIVITY: Enter the name and address of the contractor, subcontractor, grantee, Department of Defense activity or other organization *(corporate author)* issuing the report.

2a. REPORT SECURITY CLASSIFICATION: Enter the overall security classification of the report. Indicate whether "Restricted Data" is included. Marking is to be in accordance with appropriate security regulations.

2b. GROUP: Automatic downgrading is specified in DoD Directive 5200.10 and Armed Forces Industrial Manual. Enter the group number. Also, when applicable, show that optional markings have been used for Group 3 and Group 4 as authorized.

3. REPORT TITLE: Enter the complete report title in all capital letters. Titles in all cases should be unclassified. If a meaningful title cannot be selected without classification, show title classification in all capitals in parenthesis immediately following the title.

4. DESCRIPTIVE NOTES: If appropriate, enter the type of report, e.g., interim, progress, summary, annual, or final. Give the inclusive dates when a specific reporting period is covered.

5. AUTHOR(S): Enter the name(s) of author(s) as shown on or in the report. Enter last name, first name, middle initial. If military, show rank and branch of service. The name of the principal author is an absolute minimum requirement.

6. REPORT DATE: Enter the date of the report as day, month, year; or month, year. If more than one date appears on the report, use date of publication.

7a. TOTAL NUMBER OF PAGES: The total page count should follow normal pagination procedures, i.e., enter the number of pages containing information.

7b. NUMBER OF REFERENCES: Enter the total number of references cited in the report.

8a. CONTRACT OR GRANT NUMBER: If appropriate, enter the applicable number of the contract or grant under which the report was written.

8b, 8c, & 8d. PROJECT NUMBER: Enter the appropriate military department identification, such as project number, subproject number, system numbers, task number, etc.

9a. ORIGINATOR'S REPORT NUMBER(S): Enter the official report number by which the document will be identified and controlled by the originating activity. This number must be unique to this report.

9b. OTHER REPORT NUMBER(S): If the report has been assigned any other report numbers *(either by the originator or by the sponsor)*, also enter this number(s).

10. AVAILABILITY/LIMITATION NOTICES: Enter any limitations on further dissemination of the report, other than those imposed by security classification, using standard statements such as:

(1) "Distribution of this document is unlimited."

(2) "Foreign announcement and dissemination of this report by DDC is not authorized."

(3) "U. S. Government agencies may obtain copies of this report directly from DDC. Other qualified DDC users shall request through _____."

(4) "U. S. military agencies may obtain copies of this report directly from DDC. Other qualified users shall request through _____."

(5) "All distribution of this report is controlled. Qualified DDC users shall request through _____."

If the report has been furnished to the Office of Technical Services, Department of Commerce, for sale to the public, indicate this fact and enter the price, if known.

11. SUPPLEMENTARY NOTES: Use for additional explanatory notes.

12. SPONSORING MILITARY ACTIVITY: Enter the name of the departmental project office or laboratory sponsoring *(paying for)* the research and development. Include address.

13. ABSTRACT: Enter an abstract giving a brief and factual summary of the document indicative of the report, even though it may also appear elsewhere in the body of the technical report. If additional space is required, a continuation sheet shall be attached.

It is highly desirable that the abstract of classified reports be unclassified. Each paragraph of the abstract shall end with an indication of the military security classification of the information in the paragraph, represented as *(TS), (S), (C), or (U)*.

There is no limitation on the length of the abstract. However, the suggested length is from 150 to 225 words.

14. KEY WORDS: Key words are technically meaningful terms or short phrases that characterize a report and may be used as index entries for cataloging the report. Key words must be selected so that no security classification is required. Identifiers, such as equipment model designation, trade name, military project code name, geographic location, may be used as key words but will be followed by an indication of technical context. The assignment of links, roles, and weights is optional.